Correlation of functional and resting state connectivity of cerebral oxy-, deoxy-, and total hemoglobin concentration changes measured by near-infrared spectrophotometry

Ursula Wolf
Vladislav Toronov
Jee H. Choi
Rajarsi Gupta
Antonios Michalos
Enrico Gratton
Martin Wolf

Correlation of functional and resting state connectivity of cerebral oxy-, deoxy-, and total hemoglobin concentration changes measured by near-infrared spectrophotometry

Ursula Wolf,[a,b] Vladislav Toronov,[a,c] Jee H. Choi,[a,d] Rajarsi Gupta,[a] Antonios Michalos,[a,e] Enrico Gratton,[a] and Martin Wolf[a,f]

[a]University of California, Irvine, Biomedical Engineering Department, Laboratory for Fluorescence Dynamics, 3120 Natural Sciences 2, Irvine, California 92697-2715
[b]University of Bern, Institute of Complementary Medicine KIKOM, 3010 Bern, Switzerland
[c]Ryerson University, Department of Physics, Toronto, Ontario, M5B 2K3 Canada
[d]Korea Institute of Science and Technology, Center for Neural Science, Seoul, Seoul 136-791, Republic of Korea
[e]University of Illinois at Urbana-Champaign, Center for Health Information Privacy and Security, Information Trust Institute, Urbana, Illinois 61801-2307
[f]University Hospital Zurich, Neonatology, Biomedical Optics Research Laboratory, Zurich 8091 Switzerland

Abstract. The aim is to study cerebral vascular functional connectivity during motor tasks and resting state using multichannel frequency-domain near-infrared spectrophotometry. Maps of 5.7×10.8 cm size displaying changes in cerebral oxyhemoglobin (O_2Hb), deoxyhemoglobin (HHb), and total hemoglobin (tHb) concentrations were measured in the motor cortex in 12 subjects (mean age of 28.8 ± 12.7 yrs) during resting state and during two palm squeezing tasks with different timing. For each condition, phase plane plots, cross correlation functions, and connectivity indices were generated for O_2Hb, HHb, and tHb. The amplitude of the concentration changes in O_2Hb and HHb depends on the age of the subject. We found large regions of connectivity, which were similar for resting state and task conditions. This means the spatial relationships during resting state, when changes in O_2Hb, HHb, and tHb corresponded to spontaneous oscillations, were correlated to the spatial patterns during the activation tasks, when changes in O_2Hb, HHb, and tHb concentration were related to the alternation of stimulation and rest. Thus, the vascular functional connectivity was also present during resting state. The findings suggest that the vascular response to functional activation may be a nonlinear synchronization phenomenon and that resting state processes are more important than previously expected. © *2011 Society of Photo-Optical Instrumentation Engineers (SPIE)*. [DOI: 10.1117/1.3615249]

Keywords: neurovascular coupling; resting state; connectivity; near-infrared spectrophotometry; brain; functional activation; cerebral hemoglobin concentration.

Paper 11121R received Mar. 12, 2011; revised manuscript received Jul. 1, 2011; accepted for publication Jul. 1, 2011; published online Aug. 19, 2011.

1 Introduction

Functional brain activity, by neurovascular coupling, leads to changes in oxyhemoglobin (O_2Hb), deoxyhemoglobin (HHb), and total hemoglobin (tHb) concentrations. Brain activity may lead to temporally correlated changes in several regions, which are then called "connected." Three different types of connectivity were distinguished in the literature:[1,2] neuroanatomical, functional, and effective connectivity.

Neuroanatomical connectivity a,s e.g., observed by diffusion magnetic resonance tractography[3] refers to anatomical connections on the neuronal level. These connections are influenced by brain function, i.e., the plasticity of the brain enables to build or remove such connections.[1]

Functional connectivity refers to temporally correlated neurophysiologic events. We further suggest distinguishing vascular and neural functional connectivity, referring to correlations in blood circulation or neural activity, respectively. Although fluctuations in blood circulation are usually thought to be based on neural activity,[4] changes in blood circulation affect a larger area of the brain than the region of neuronal activity itself,[5,6] which suggests that vascular and neuronal functional connectivity have spatially different patterns. Vascular functional connectivity (VFC) can be measured by magnetic resonance imaging (MRI BOLD signal),[4] positron emission tomography, or near-infrared spectrophotometry (NIRS). NIRS allows measuring O_2Hb, tHb, and HHb at relatively high time resolution over an extended area of the brain. Neural functional connectivity can be measured by EEG and MEG.[7]

Effective connectivity refers to the influence that one neural system exerts over another system. Thus, this term is similar to the term "functional connectivity," except that here a causal relationship is included.

Cerebral blood perfusion shows spontaneous oscillations in resting state, which affects O_2Hb, HHb, and tHb concentrations.[8] Resting state oscillations have also been extensively analyzed using the BOLD signal of functional magnetic

resonance imaging (fMRI) (see review in Ref. [9]). Since task related changes in neuronal metabolism are small ($<5\%$), when compared to resting state metabolism, it was suggested that the resting state oscillations may significantly influence the VFC and that further studies to investigate the interplay of resting state related and task related VFC are needed.[9] Using NIRS, resting state oscillations were already shown to significantly influence the neurovascular response to functional stimulation.[10] Therefore, the first aim of this study was to compare VFC of resting state oscillations and hemodynamic changes evoked by brain activation.

Previous studies using the BOLD-signal of fMRI, which represents the HHb, suggest that regions with VFC also exhibit similar connectivity of the spontaneous oscillations during rest.[4] There are two possible explanations for this similarity: VFC as of vascular origin reflects the structures of the vasculature and/or since the mind is also active during rest, this activity through neurovascular coupling will lead to hemodynamic changes, which display a similar connectivity to the one during activation. References [11] and [4] suggest that the latter is the case.

The second aim in the present study was to obtain a more complete picture of vascular function by including O_2Hb and tHb, in addition to HHb. This also enables us to study the correlation between O_2Hb and HHb, which is part of VFC. We used multichannel frequency-domain near-infrared spectrophotometry to generate functional maps of the brain during motor stimulation and rest. Patterns of O_2Hb, HHb, and tHb changes between locations within the mapped region during stimulation, and rest were analyzed using phase plane plots, cross correlation functions, correlations coefficients, connectivity analyses, and calculations of time lags between locations.

2 Materials and Methods

2.1 Instrument

We used a frequency-domain near-infrared spectrophotometer (Omnia ISS Inc.), which was previously described.[12] The light of 16 laser diodes (8/wavelength) at 830 and 758 nm, respectively, is intensity modulated at 110,000 kHz. The laser diodes are time multiplexed, i.e., only one laser diode is on at a given time, and their light is focused by a gradient index lens into glass fibers of a 400-μm diameter, which guide the light to the tissue. The light is detected by two glass fibers of 3-mm diameter and conducted back to the instrument, where it is collected in two photomultiplier tube detectors. The high voltage and consequently, the amplification of the photomultipliers, is modulated at a frequency of 110,005 kHz frequency. This heterodyning demodulates the high frequency and the resulting frequency of 5 kHz is recorded and by time locked fast Fourier transform (FFT), the mean intensity (dc), modulation amplitude (ac), and phase (Φ) of the detected light are determined.

The geometry of the sensor consists of two partly overlapping circles at a radius of 3 cm. In each circle center, a detector is placed and the source pairs (both wavelengths per pair) are arranged along the circular arc equidistantly to the corresponding detector (Fig. [1]). This arrangement provides 10 bi-wavelength source detector channels. The laser diodes were sequentially multiplexed at 100 Hz to permit discrimination between different channels and wavelengths at each detector. The sample rate for an entire map was 6.25 Hz.
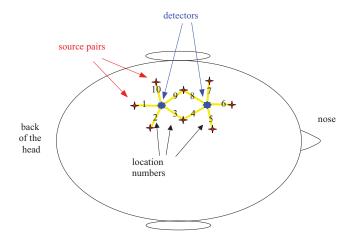

Fig. 1 The light sources are arranged in two circles of 3 cm radius around the two detector fibers. Thus, an area of 5.7×10.8 cm is investigated with a spatial resolution of 10 pixels.

2.2 Measurement Protocol

The sensor was placed on the subject's head above the motor cortex (C3 or C4 position,[13] depending on the subject's handiness) contralateral to the exercising hand. All subjects except one were right-handed.

After 5 min of baseline, the subjects performed two different palm-squeezing tasks at a palm-squeezing frequency of approximately 1.4 Hz. Each task consisted of alternating stimulation and rest periods, which were repeated 10 times. During the first task, the subject was palm-squeezing for 21 s and resting for 20 s (total duration 430 s), and during the second task was palm-squeezing for 10 s and resting for 17 s (total duration 297 s). Two different timings were chosen to examine their potential effect on VFC, since they may affect the vascular functional response. The specific values of the timing were chosen because they showed clear functional activation in a previous study.[10]

The protocol was approved by the Institutional Review Board of the University of Illinois at Urbana–Champaign (No. 94125), where the study was carried out.

2.3 Data Analysis

The optical raw data (dc) was converted to O_2Hb, HHb, and tHb by using the differential pathlength factor (DPF)-method:[14] In the first step, the natural logarithm of the dc values was taken. Then, the mean value of the complete measurement was subtracted to receive I. I was divided by the sources detector distance r and the respective $\mathrm{DPF}_{758\,nm} = 6.32$ and $\mathrm{DPF}_{830\,nm} = 5.64$. These DPF values are based on their own measurements. O_2Hb and HHb were calculated according to the following equation:

$$
\begin{bmatrix} \mathrm{HHb} \\ \mathrm{O_2Hb} \end{bmatrix}
= 1000 * \begin{bmatrix} -0.3674 & +0.2342 \\ +0.2843 & -0.6131 \end{bmatrix} * \begin{bmatrix} I_{758nm}/r/\mathrm{DPF}_{758nm} \\ I_{830nm}/r/\mathrm{DPF}_{830nm} \end{bmatrix},
$$
$$(1)$$

tHb corresponds to the sum of O_2Hb and HHb.

The O_2Hb, HHb, and tHb data were low-pass filtered (cut-off 0.1 Hz) to remove arterial pulsations and effects of breathing, and to focus on spontaneous low-frequency fluctuations.[15] The filter was a digital symmetric window low pass filter, specifically designed not to introduce any phase shifts. Data were visually inspected for movement artifacts, which were manually removed.

2.3.1 Phase plane plots

The data were detrended by subtracting a moving average of a period of 41 s (baseline and task 1) or 27 s (task 2), and each trace was normalized to the standard deviation of the oscillations to simplify scaling and time lag calculation. Phase plane plots for O_2Hb, HHb, and tHb were generated by setting the signal at location 1 as a reference or seed (Fig. 1) for all other locations. The phase plane plots display the reference location (x-axis) versus the signal at a specific other location (y-axis). Similar figures were also plotted for O_2Hb (y-axis) versus HHb (x-axis). Plots were generated separately for the three conditions: Baseline, task 1, and task 2.

2.3.2 Time lag and coherence between locations

Time lags between two traces of a specific phase plane plot were determined numerically. One trace was shifted with respect to the other in consecutive steps of 0.16 s from a total shift of -10 to $+10$ s. For each step of time shift the mean deviation (MD) of the data points from the 45º and 135º line (i.e., the mean thickness of the pattern with respect to that line) in the particular phase plane plot was calculated. If two traces are in phase, which is the case for O_2Hb plots (Fig. 2) and HHb plots (Fig. 3), their MD will have a minimum ideally at the 45º line. If the two traces are in antiphase, which was found for O_2Hb versus HHb plots (Fig. 4), the minimum will ideally occur at the 135º line. The step of time shift with the minimum deviation represents the time lag.

2.3.3 Cross correlation function and correlation coefficient

Cross correlation functions were calculated between the seed location (location 1 in Fig. 1) and other locations. The correlation coefficient was determined as a numerical measure of coherence, where the value "1" indicates perfect coherence and "0" no coherence. Correlation coefficients were calculated for all possible combinations within a map.

2.3.4 Activation patterns

To determine the spatial pattern of the activation, at each location the mean difference between palm squeezing periods and rest periods was calculated for O_2Hb, HHb, and tHb. To detect activated regions, we set the following thresholds for concentration changes: $\triangle O_2Hb > 0.2 \ \mu m/l$, $\triangle HHb < -0.1 \ \mu m/l$, and $\triangle tHb > 0.2 \ \mu m/l$. The size of the threshold was selected similar to the previously used ones.[16] Compared to a statistical test and taking a p-value as an identifier for brain activation, setting an amplitude threshold has the advantage that it is more independent of physiological background noise, which varies between subjects.

2.3.5 Connectivity

We determined the connectivity according to Ref. 17. Activated regions were detected as mentioned above (Sec. 2.3.4). Two types of connectivity were calculated:

1. Functionally related connectivity (FRC): If two signals at two locations were within an activated region during a task condition and had a correlation coefficient of $r^2 > 0.5$ during baseline condition, they were considered as connected. The percentage of such connected signals is the FRC.

2. Functionally unrelated connectivity (FUC): Furthermore, we calculated the percentage of connected signals, when only one of the signals was within an activated area and the other was not. This yielded the relation between activated and nonactivated regions during baseline.

To set the magnitude of the connectivity between task 1 and baseline in relation, we also calculated the connectivity between task 1 and task 2.

2.3.6 MRI scans

To test for a potential influence of superficial tissue on the amplitude of the measured NIRS signals, the thickness of skin and skull and the distance between the surface of the head and the brain were measured on coronal anatomical T1-weighted scans obtained by a 1.5 T MR scanner (Sigma General Electric Medical Systems, Milwaukee, Wisconsin). Multimodality radiological markers (IZI Medical Products Corp., Baltimore, Maryland), detectable by MRI, indicated the position of the optical sensor. All three distances were measured using standard imaging software at three locations below the optical sensor and averaged.

2.3.7 Statistics

The correlation between patterns or parameters was tested using Pearson's correlation coefficient for linear relations and the Spearman's rho for nonlinear correlations as indicated (statistical software: SPSS 11.0). The patterns of O_2Hb versus HHb (Fig. 7) were compared by calculating the correlation coefficient between two conditions (i.e., baseline versus task 1 or baseline versus task 2) for all subjects at a specific location.

3 Subjects

Twelve healthy volunteers (11 male, 1 female) with a mean age of 28.8 ± 12.7 (range 18 to 60) yrs were included in the study after written informed consent was obtained. MRI data was available for 8 subjects.

4 Results

Phase plane plots of maps of the two tasks and baseline are shown in Figs. 2, 3, and 4.

The resting state slow oscillations in O_2Hb at baseline express a similar pattern in various locations of the map, indicating a VFC (Fig. 2 baseline). During stimulation periods, despite a change in the frequency of the oscillation, the VFC between the locations is maintained (Fig. 2 task 1 and 2). Functional
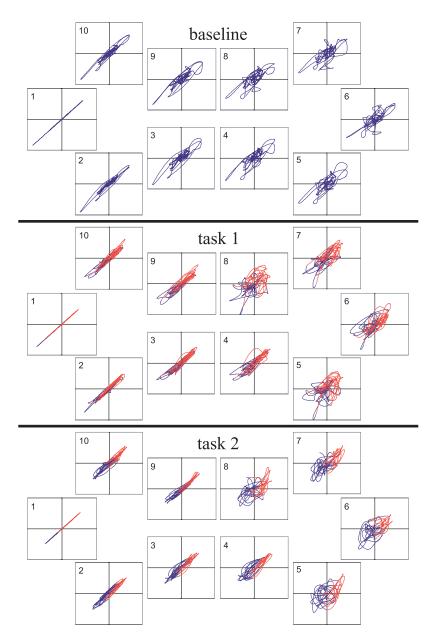
Fig. 2 Maps of phase plane plots depicting the changes in O_2Hb during baseline recording, Task 1 and 2 from a 60 yr old subject. The arrangement of the phase plane plots represents the location on the head as shown in Fig. 1. The O_2Hb of the leftmost figure was used as a reference for all x-axis values and therefore, represents a straight line. Independent of the task, it can clearly be seen that the phase plane plots close to the reference are approximately straight lines and therefore in good correlation and almost in phase with the reference. The broadening of the figures to an ellipse represents a phase shift. Toward the right-side, four figures appear round and more chaotic, which shows that the correlation to the reference is lost. The light gray (red) part of the traces in the figure represents the O_2Hb level during the palm squeezing task, and the dark gray (blue) the traces during rest. Thus, it can be seen that there is a distinct polarity of the palm squeezing task and the rest periods especially for the left-side with the good correlation. A separation of the two shades of gray (colors) in the vertical direction indicates an activation at the specific location, while a separation in the horizontal direction indicates an activation at the reference location. Thus, in task 2 a distinct activation occurs across the whole map, which is in contrast to task 1. Each plot is 8 standard deviations (± 4) high and wide.

activity can clearly be discerned by the light gray (red) part of the trace in the plot (during stimulation) in contrast to the dark gray (blue) part (during rest). A similar but not congruent pattern is found for HHb although the VFC is less pronounced (Fig. 3). The high VFC is confirmed by a mean $\pm$ standard deviation correlation coefficient across maps and subjects of $r^2 = 0.52 \pm 0.29$ for O_2Hb, $r^2 = 0.23 \pm 0.24$ for HHb, and $r^2 = 0.62 \pm 0.27$ for tHb. The difference in the correlation coefficient between tasks and baseline is less than 3% and is thus minimal.

The cross correlation functions displayed in Figs. 5 and 6 are another valuable method to demonstrate the spatial coherence of the hemodynamic changes.

Table 1 shows the connectivity. The results demonstrate a high FRC for O_2Hb and tHb, while the FRC for HHb is much lower. Comparing the FRC between the two tasks yields similar values as comparing task with baseline. FUC yields generally approximately 25% lower values than FRC. This indicates that functionally connected areas during a task also remain more connected during resting state, but not to the same degree. The
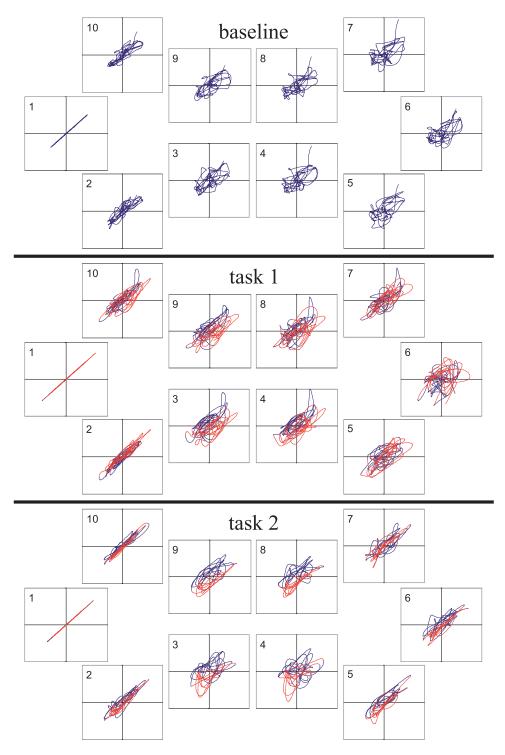
Fig. 3 Maps of phase plane plots of the concentration changes in HHb, which are from the same subject as in Fig. 2 and have an analogous format. The HHb pattern is different from the O_2Hb pattern and shows coherences for the three leftmost phase plane plots.

high FUC values for O_2Hb and tHb imply a substantial coherence across a relatively large area of the brain, which is independent of the area activated by the stimulation.

When plotting O_2Hb versus HHb (Fig. 7), anti-correlation patterns are revealed. There is a significant correlation between these patterns during baseline and task 1 ($r^2 = 0.53 \pm 0.18$, $p < 0.05$ in 9 out of 10 locations), and baseline and task 2 [$r^2 = 0.49 \pm 0.21$ ($p < 0.05$ in 7 out of 10 locations)].

The time lags between locations are small (<1 s) in the case of a high coherence (MD < 0.5). The time lag gives information about the temporal succession between the regions, i.e., how a concentration change spreads throughout the brain.

The degree of spatial (negative) correlation between O_2Hb and HHb depends significantly ($p = 0.008$ Spearman) on the age of the subject. Further analysis shows a highly significant nonlinear correlation between age and amplitude of the changes in O_2Hb ($p = 0.00004$) or HHb ($p = 0.00038$) (Fig. 8). The fact that this effect is not due to a change of the anatomical
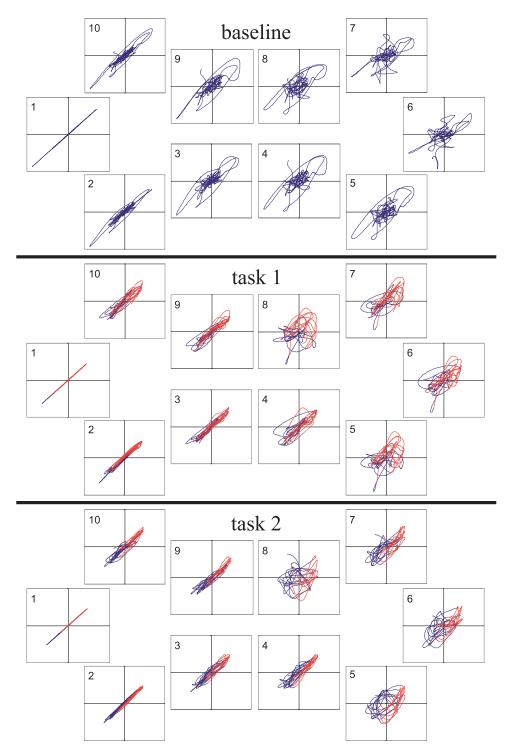
Fig. 4 Maps of phase plane plots of the concentration changes in tHb, which are from the same subject as in Fig. 2 and have an analogous format. These maps are similar to the ones displayed in Fig. 2, because O_2Hb constitutes a major part of the tHb.

thickness of the skin, skull, and the distance from the surface of the head to the brain with age was demonstrated by the correlation analysis (Pearson and Spearman) comparing these thicknesses with the amplitude of the O_2Hb and HHb, which did not show significances. Furthermore, the amplitudes of the signals are not significantly different between baseline and task. Mean thickness was 2.87 ± 0.45 mm for skin, 2.98 ± 0.74 mm for the skull, and 13.58 ± 1.13 mm for the distance from the surface of the head to the brain.

5 Discussion

5.1 Correlation of Resting State and Task Related VFC

Maps of changes in O_2Hb, tHb, and HHb in the brain obtained by frequency-domain near-infrared spectrophotometry were analyzed by phase plane plots and cross correlation. These are two model-based methods, which require a seed pixel as a reference. There is a variety of other methods for
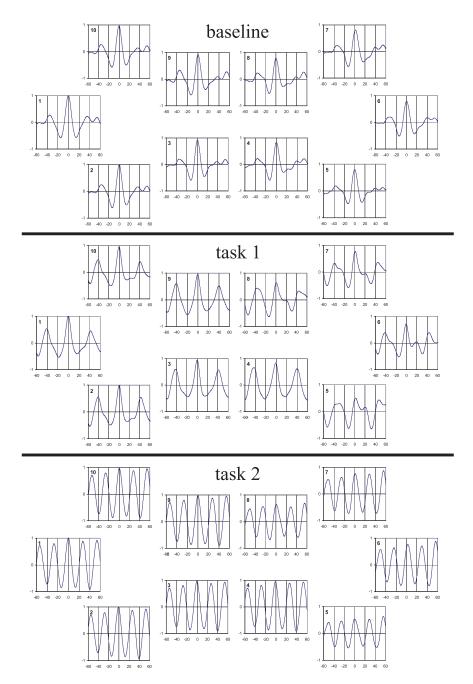
Fig. 5 Cross correlation function of O_2Hb for the same subject and set-up as in Fig. 2. The peak at 0 s corresponds to the correlation coefficient (r not squared). When the peak has a maximum, which is not at 0 s, there is a time lag between this specific location and the reference location (location 1). The height of the peak indicates the degree of correlation between the two locations. Secondary peaks at other time lags (e.g., at ± 41 s for task 1 and at ± 27 s for task 2) indicate a prevailing periodicity of the signal (e.g., period of stimulation and rest of the two tasks). If there is no well-defined periodicity, which is the case for slow oscillations during baseline, the secondary peaks will be smaller. At reference location 1, the two cross correlated functions are identical and thus this corresponds to an autocorrelation function. The cross correlation functions show that during baseline similar periodicities are found as during task 1 and that during task 2, mainly the task related periodicities appear, while the resting state oscillations are not visible. This demonstrates an interaction of the two signals. The cross correlation functions for tHb are similar to the ones of O_2Hb and are therefore not displayed.

VFC; their advantages and limitations are described in recent reviews.[18,19]

For resting state oscillations, previous publications[8] used the conventional FFT, which is not accurate when the frequency of the observed signal is not constant, which is true for resting state oscillations, and when the signal has a low frequency and contains only a few periods, which is true for the functional tasks. Thus, in our study, the amplitude of the resting state oscillation was not significantly different from the one due to functional activation, while Ref. 8 suggests that the amplitude due to activation is approximately twice as high as the one of resting state oscillations. This may be an artifact, because the frequency of resting state oscillations is not constant, which leads to a broadening of the peak in the FFT and consequently
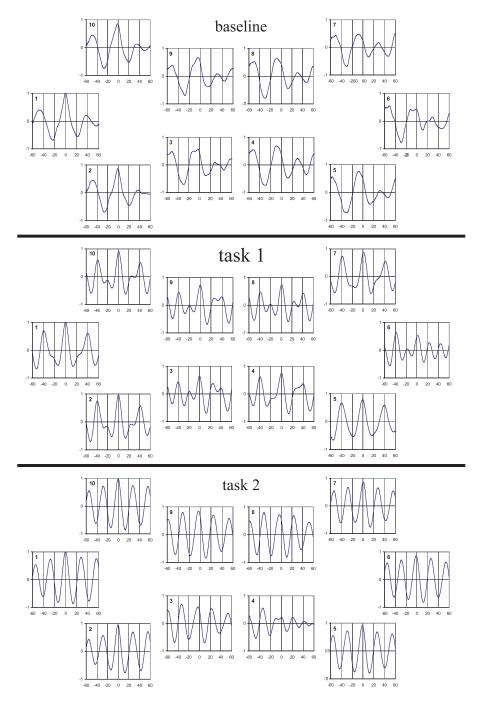
Fig. 6 Cross correlation functions of HHb for the same subject and set-up as in Fig. 2.

falsely low amplitude. The same is true for the cross corre-lation function, whose secondary peaks are diminished, when the frequency is not constant. Therefore, we chose phase plane plots that are not influenced by a changing periodicity, and are therefore excellent tools to analyze the patterns of functional maps. In addition, phase plane plots are user-friendly, because, after a short period of acquaintance, they present the important information and quality of the data in a comprehensible way.

Other studies using NIRS used appropriate seed-based cor-relation analysis and cluster analysis to analyze resting state connectivity in the sensorimotor and auditory cortex region and found robust maps of connectivity, which were in line with pre-vious fMRI findings and thus were considered as a validation of the validity of NIRS.[20]

Another advantage of the phase plane plots is that they dis-play the whole evolution of the signal rather than averaged mea-surement. This enables one to detect movement artifacts and irregularities at once, while they can be hidden in block aver-aged data or cross correlation functions.

Furthermore, the separate coloring of the stimulation and rest periods, which can clearly be seen in Figs. 2, 3, and 4 makes activation visible.

A time lag leads to a broadening of the phase plane plots. For small delays, the plots become ellipsoid, while for delays of
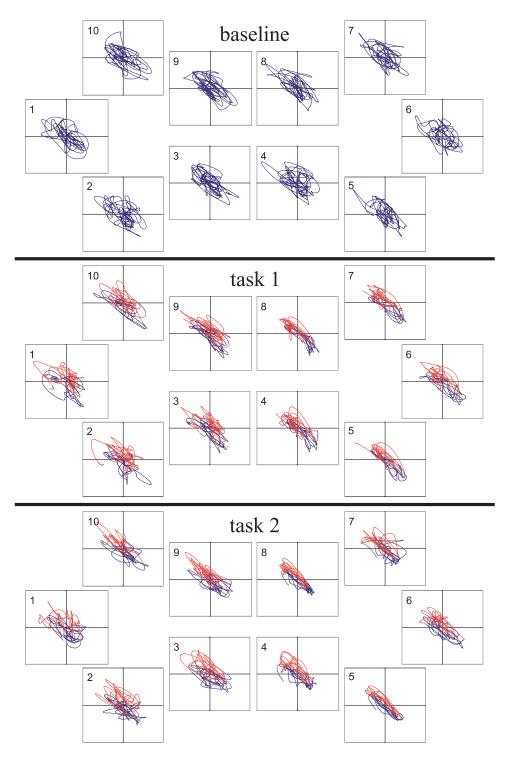
Fig. 7 The O_2Hb on the *y*-axis was plotted versus the HHb on the *x*-axis. Between O_2Hb and HHb, a negative correlation is revealed, which is strong in this 22 yr old subject compared to older subjects.

a period of $\pi/2$ the plots become circular. These can easily be distinguished from chaotic plots (e.g., Fig. 2, task 2, locations 5, 6, and 8), which represent poor correlation.

Concerning the size of the regions of coherence, e.g., for tHb the mean $r^2 \pm$ standard deviation of 0.62 ± 0.27 means that there was in average 62% of agreement between the seed pixel and other pixels. A value of $r^2 = 1.0$ indicated that all pixels correlated perfectly with the seed pixel, while a value of $r^2 = 0.0$

indicated that the changes in tHb were completely uncorrelated between the seed pixel and the other pixels. Considering that the region of connectivity is limited, it is expected, and indeed the case, that a proportion of the pixels is not or little correlated with the seed pixel. The mean $r^2 = 0.62$ indicates that there are considerable regions of high correlation. A high $r^2 \geq 0.8$ ($r^2 \geq 0.6$) was found in 22 (46), 3 (10), and 33% (63%) of the pixels for O_2Hb, HHb, and tHb, respectively. Except for HHb,

Table 1 The results of the connectivity analysis for O_2Hb, HHb, and tHb.

		Connectivity		
Type of connectivity	Comparison	O_2Hb in%	HHb in%	tHb in%
Within region of functional activation	Task 1 to baseline	66.9	26.1	90.5
	Task 2 to baseline	93.6	27.3	100.0
	Task 1 to task 2	73.4	32.4	89.4
Between region of functional activation and region without activation	Task 1 to baseline	59.7	2.2	74.4
	Task 2 to baseline	49.6	9.3	62.0
	Task 1 to task 2	55.8	7.4	67.4

this indicates that considerable regions of high coherence were found.

These regions were very similar during baseline compared to task periods. Not even the amplitude was significantly affected by the condition. This similarity between resting state and task related patterns is remarkable (Figs. 2 and 3, and 4). However, in the same figures, it is also quite obvious that these regions were not congruent with the regions of functional activity.

Resting state oscillations have been extensively analyzed using the BOLD signal of fMRI (see review in Ref. 9) and also in studies by NIRS, e.g., in the motor cortex region[20] or larger regions of the brain.[21] Since task related changes in neuronal metabolism are small ($<5\%$), when compared to resting state
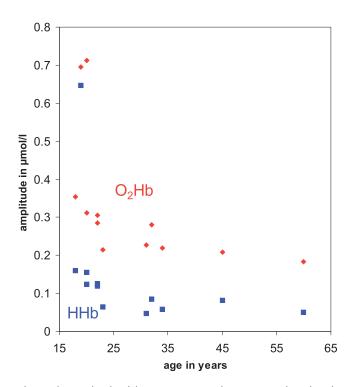
metabolism,[9] it is not surprising that there is quite a degree of similarity between VFC during resting state and functional task, which is what we find. This resting state VFC may be more important than the task related VFC. Since the BOLD signal is limited to the HHb only, our data delivers the complete hemodynamic change by providing O_2Hb and tHb, in addition to HHb.

What is the origin of this resting state VFC? It could either be due to structural connectivity, i.e., the structure of the blood vessels, or it is a functional connectivity component reflected by the similarity between brain activity during resting state and motor stimulation. So far in reviews,[4,9] the favored hypothesis that functional activity is the origin and supportive direct and indirect evidence for a neural basis of resting state slow oscillations is cited. Surprisingly, the possibility that the structure of the tree of blood vessels may contribute to this VFC is little considered. The fact that regions of a high degree of connectivity also show small time lags may indicate that the role of this structural connectivity based on the vasculature and not neurons, may be underestimated.

5.2 Functionally Related and Unrelated Connectivity

The FRC was higher than the FUC, which indicates that there is a significant relation between the functional hemodynamic changes and the resting state slow oscillations. This can be interpreted, according to Ref. 10, as hemodynamic oscillations that are present with considerably variable frequencies during resting state. Motor stimulation leads to a synchronization of these resting state oscillations with the stimulation events. The degree of synchronization depends on the frequency of the stimulation and HHb is more significantly affected than O_2Hb. This is an effect well-known in nonlinear systems (frequency pulling). This means that functional cerebral hemodynamics can also be considered as a nonlinear synchronization phenomenon.

The coherence patterns and the connectivity were considerably lower for HHb. This may be due to physiological differences, i.e., HHb is more affected by oxygen consumption than O_2Hb and may imply that HHb is a better indicator for activation than O_2Hb. However, O_2Hb is generally considered to be

Fig. 8 The amplitude of the concentration change in O_2Hb and HHb significantly depended highly on the age.

the most reliable indicator for functional brain activity in the NIRS literature,[6] because it has a higher amplitude and contains the same information. Thus, in Fig. 7, it is obvious that O_2Hb displays the inverted pattern of the HHb. Since the amplitude of the HHb signal is smaller than for the O_2Hb signal, the HHb signal is more affected by noise. This is likely to derogate the detection of the connectivity in our data presented in Table 1.

Our results are in contrast to Refs. 11 and 17, who found a much higher FRC and much lower FUC than in our data, but without measuring O_2Hb or tHb. There are several possible reasons for this discrepancy. Since NIRS quantifies concentration changes, we are able to set threshold values for changes in HHb of < -0.1 μm/l, which is comparable between subjects. Thus, Refs. 11 and 17 relied on a correlation coefficient >0.35 when comparing the BOLD-signal to a square wave function, which represented the task.

Compared to Refs. 11 and 17, we investigated only one cerebral hemisphere, a smaller area of cerebral tissue around the motor cortex, and specifically superficial layers of cerebral tissue. Our instrument had a lower spatial resolution. These factors may explain the higher percentage for the FUC.

In addition, the connectivity widely depends on the thresholds set for the correlation coefficients and for the concentration changes. Generally, higher threshold values lead to smaller areas of detected activity and a higher FRC and lower FUC. This indicates that indeed during baseline, areas of the motor cortex remain connected. The largest difference between FRC and FUC of approximately 65% was found in O_2Hb for a functional change >0.4 μm/l and $r^2 > 0.75$.

5.3 The Effect of Age

The coherence in the O_2Hb versus HHb plots was less distinct in older subjects compared to younger subjects. This new finding may be either an interesting physiological feature or be due to a smaller amplitude of the signal in older subjects, i.e., a matter of signal-to-noise ratio. What is the origin of the higher amplitude in younger subjects?

Reference 22 found an age dependence of the DPF, which is used to calculate O_2Hb, HHb, and tHb. When this age-dependence was taken into account, the age dependent effect in our data was more pronounced and the significance increased approximately threefold. Thus, changes in optical properties with age are not an explanation.

To test whether the effect may be related to anatomical differences depending on the age, e.g., a different thickness of the skin, skull, and distance to the brain, which would affect the path of light, we measured the thickness of these layers using MRI. No significant correlation between the anatomical features and the amplitude of the O_2Hb and HHb oscillations was found.

There is a cognitive decline with age.[23] Older people also use different areas of the brain than younger people,[24] which may imply that the functional networks change. Thus, different levels of brain activity with age may very well explain the difference.

In addition, the cerebral blood vessels decline as well. The stiffness of arteries increases.[25] This reduced elasticity may be a vascular explanation for the reduced amplitude with age.

It has to be kept in mind that this study was not designed to detect an age-related effect, and such effect was not expected before conducting the study. The effect was discovered when analyzing the data. Consequently, the subjects are not evenly distributed between the different ages, and there are only two subjects older than 35 years of age. However, even if these subjects are removed from the data, a highly significant age-related effect persists. To corroborate these results, it will be necessary to reproduce the effect in a group of subjects with evenly distributed ages.

5.4 Limitations of the Study

The current set-up with only two detector locations, which was chosen according to instrumental factors, may lead to crosstalk. If there is an optical change directly below the detector, this will appear like a change in the whole area around the detector. This type of artifact would lead to identical signals in all channels of one detector, which in addition should have no time lag. In practice, these two conditions were never fulfilled and we can thus exclude this artifact.

In order to achieve a higher signal-to-noise ratio, it may be more effective to use stimulation and rest periods that are not constant. This may reduce noise, because constant periods can be subject to resonance effects, frequency pulling, and are more likely to coincide with physiological frequencies. Variable periods are used to study evoked potentials by EEG.

It has been shown that the resting state VFC depends on the frequency band chosen.[21] Due to its potentially high time resolution, NIRS is an excellent tool to study these properties. The current study focused on frequencies between 0.014 to 0.1 Hz and the two specific frequencies elicited by the functional activation tasks in our study. No frequency specific connectivity was found.

The effect of systemic parameters such as changes in blood pressure was not assessed in this study. Changes in systemic blood pressure may contribute to cerebral hemodynamics both during resting state,[26] as well as during the stimulation task,[27] which could lead to an overestimation of VFC. Since our results show localized patterns of VFC, such a systemic effect, which has to be generalized, is unlikely to have played a decisive role. However, in future studies systemic parameters should be taken into consideration.

6 Conclusion

Using phase plane plots and cross correlation functions VFC was analyzed during functional stimulation tasks and in resting state. The main findings of this study are relatively large regions of VFC (up to 10 cm length), which were independent of the motor stimulation task. The FRC is approximately 25% higher than the FUC, which indicates that the activated part of the motor cortex remains functionally connected even during baseline. O_2Hb and tHb, whose FCR was not determined previously, have a much higher FRC and FUC than HHb. The findings also suggest that the vascular response to functional activation is a nonlinear synchronization phenomenon. The amplitude of the concentration changes in O_2Hb and HHb depends on the age of the subject.

References

1. A. A. Fingelkurts and S. Kahkonen, "Functional connectivity in the brain–is it an elusive concept?," *Neurosci. Biobehav. Rev.* **28**(8), 827–836 (2005).
2. L. Lee, L. M. Harrison, and A. Mechelli, "The Functional Brain Connectivity Workshop: report and commentary," *Network* **14**(2), R1–15 (2003).
3. M. Guye, F. Bartolomei, and J. P. Ranjeva, "Imaging structural and functional connectivity: towards a unified definition of human brain organization?," *Curr. Opin. Neurol.* **21**(4), 393–403 (2008).
4. D. P. Auer, "Spontaneous low-frequency blood oxygenation level-dependent fluctuations and functional connectivity analysis of the 'resting' brain," *Magn. Reson. Imaging* **26**(7), 1055–1064 (2008).
5. D. Malonek and A. Grinvald, "Interactions between electrical activity and cortical microcirculation revealed by imaging spectroscopy: implications for functional brain mapping," *Science* **272**(5261), 551–554 (1996).
6. M. Wolf, M. Ferrari, and V. Quaresima, "Progress of near-infrared spectroscopy and topography for brain and muscle clinical applications," *J. Biomed. Opt.* **12**(6), 062104 (2007).
7. J. M. Schoffelen and J. Gross, "Source connectivity analysis with MEG and EEG," *Hum. Brain Mapp.* **30**(6), 1857–1865 (2009).
8. H. Obrig, M. Neufang, R. Wenzel, M. Kohl, J. Steinbrink, K. Einhaupl, and A. Villringer, "Spontaneous low frequency oscillations of cerebral hemodynamics and metabolism in human adults," *Neuroimage* **12**(6), 623–639 (2000).
9. M. D. Fox and M. E. Raichle, "Spontaneous fluctuations in brain activity observed with functional magnetic resonance imaging," *Nat. Rev. Neurosci.* **8**(9), 700–711 (2007).
10. V. Toronov, M. A. Franceschini, M. Filiaci, S. Fantini, M. Wolf, A. Michalos, and E. Gratton, "Near-infrared study of fluctuations in cerebral hemodynamics during rest and motor stimulation: temporal analysis and spatial mapping," *Med. Phys.* **27**(4), 801–815 (2000).
11. B. Biswal, A. G. Hudetz, F. Z. Yetkin, V. M. Haughton, and J. S. Hyde, "Hypercapnia reversibly suppresses low-frequency fluctuations in the human motor cortex during rest using echo-planar MRI," *J. Cereb. Blood Flow Metab.* **17**(3), 301–308 (1997).
12. S. Fantini, M. A. Franceschini, J. S. Maier, S. A. Walker, B. Barbieri, and E. Gratton, "Frequency-domain multichannel optical detector for noninvasive tissue spectroscopy and oximetry," *Opt. Eng.* **34**, 32–42 (1995).
13. H. H. Jasper, "Report of the committee on methods of clinical examination in electroencephalography," *Electroencephalogr. Clin. Neurophysiol.* **10**, 370–375 (1957).
14. D. T. Delpy, M. Cope, P. van der Zee, S. Arridge, S. Wray, and J. Wyatt, "Estimation of optical pathlength through tissue from direct time of flight measurement," *Phys. Med. Biol.* **33**(12), 1433–1442 (1988).
15. B. B. Biswal, M. Mennes, X. N. Zuo, S. Gohel, C. Kelly, S. M. Smith, C. F. Beckmann, J. S. Adelstein, R. L. Buckner, S. Colcombe, A. M. Dogonowski, M. Ernst, D. Fair, M. Hampson, M. J. Hoptman, J. S. Hyde, V. J. Kiviniemi, R. Kotter, S. J. Li, C. P. Lin, M. J. Lowe, C. Mackay, D. J. Madden, K. H. Madsen, D. S. Margulies, H. S. Mayberg, K. McMahon, C. S. Monk, S. H. Mostofsky, B. J. Nagel, J. J. Pekar, S. J. Peltier, S. E. Petersen, V. Riedl, S. A. Rombouts, B. Rypma, B. L. Schlaggar, S. Schmidt, R. D. Seidler, G. J. Siegle, C. Sorg, G. J. Teng, J. Veijola, A. Villringer, M. Walter, L. Wang, X. C. Weng, S. Whitfield-Gabrieli, P. Williamson, C. Windischberger, Y. F. Zang, H. Y. Zhang, F. X. Castellanos, and M. P. Milham, "Toward discovery science of human brain function," *Proc. Natl. Acad. Sci. U.S.A.* **107**(10), 4734–4739 (2010).
16. M. Wolf, U. Wolf, V. Toronov, A. Michalos, L. A. Paunescu, J. H. Choi, and E. Gratton, "Different time evolution of oxyhemoglobin and deoxyhemoglobin concentration changes in the visual and motor cortices during functional stimulation: a near-infrared spectroscopy study," *Neuroimage* **16**(3 Pt 1), 704–712 (2002).
17. B. Biswal, F. Z. Yetkin, V. M. Haughton, and J. S. Hyde, "Functional connectivity in the motor cortex of resting human brain using echo-planar MRI," *Magn. Reson. Med.* **34**(4), 537–541 (1995).
18. K. Li, L. Guo, J. Nie, G. Li, and T. Liu, "Review of methods for functional brain connectivity detection using fMRI," *Comput. Med. Imaging Graph* **33**(2), 131–139 (2009).
19. N. Ramnani, T. E. Behrens, W. Penny, and P. M. Matthews, "New approaches for exploring anatomical and functional connectivity in the human brain," *Biol. Psychiatry* **56**(9), 613–619 (2004).
20. C. M. Lu, Y. J. Zhang, B. B. Biswal, Y. F. Zang, D. L. Peng, and C. Z. Zhu, "Use of fNIRS to assess resting state functional connectivity," *J. Neurosci. Methods* **186**(2), 242–249 (2010).
21. S. Sasai, F. Homae, H. Watanabe, and G. Taga, "Frequency-specific functional connectivity in the brain during resting state revealed by NIRS," *Neuroimage* **56**(1), 252–257 (2011).
22. A. Duncan, J. H. Meek, M. Clemence, C. E. Elwell, P. Fallon, L. Tyszczuk, M. Cope, and D. T. Delpy, "Measurement of cranial optical path length as a function of age using phase resolved near infrared spectroscopy," *Pediatr. Res.* **39**(5), 889–894 (1996).
23. S. A. Small, "Age-related memory decline: current concepts and future directions," *Arch. Neurol.* **58**(3), 360–364 (2001).
24. C. L. Grady, "Functional brain imaging and age-related changes in cognition," *Biol. Psychol.* **54**(1–3), 259–281 (2000).
25. M. F. O'Rourke, "Arterial aging: pathophysiological principles," *Vasc. Med.* **12**(4), 329–341 (2007).
26. R. C. Mesquita, M. A. Franceschini, and D. A. Boas, "Resting state functional connectivity of the whole head with near-infrared spectroscopy," *Biomed. Opt. Express* **1**(1), 324–336 (2010).
27. I. Tachtsidis, T. S. Leung, M. M. Tisdall, P. Devendra, M. Smith, D. T. Delpy, and C. E. Elwell, "Investigation of frontal cortex, motor cortex and systemic haemodynamic changes during anagram solving," *Adv. Exp. Med. Biol.* **614**, 21–28 (2008).